Breakup Characteristics of Impinging and Swirl Type Injectors

윤 영 빈 *
Y. B. Yoon

ABSTRACT

The breakup characteristics of liquid sheets formed by the impinging and swirl type injectors were studied as increasing the Weber number (or injection condition) and the ambient gas pressure up to $4.0MPa$. In the case of impinging type injector, we compared the changes of breakup lengths between laminar and turbulent sheets, which are formed by the impingement of laminar and turbulent jets, respectively. The results showed that both sheets expand as increasing the injection velocity irrespective of the ambient gas density when the gas based Weber number is low. When the Weber number is high, however, the breakup of turbulent sheet depends on the hydraulic force of jets as well as the aerodynamic force of ambient gas which determines the breakup of laminar sheet. Using the experimental results, we could suggest empirical models on the breakup lengths of laminar and turbulent sheets. In the case of swirl type injector, as We_l and ambient gas density increased, the disturbances on the annular liquid sheet surface were amplified by the increase of the aerodynamic forces, and thus the liquid sheet disintegrated near from the injector exit. Finally, the measured breakup length of swirl type injector according to the ambient gas density and We_l was compared with the result by the linear instability theory. We found that the corrected breakup length relation derived from linear instability theory considering the attenuation of sheet thickness agrees well with our experimental results.

Keywords: Breakup Characteristics, Breakup Length, Impinging Type Injector, Swirl Type Injector, Linear Instability Theory

1. INTRODUCTION

Impinging type injectors that atomize liquid mass into fine drops using the impinging momentum of liquid jets are commonly used in liquid rocket engines due to their advantages: low manufacturing cost, potentially high flow rate, compatibility of chamber wall and so forth [1]. Impinging type injectors basically form a liquid sheet when two or more liquid jets impinge at a point. The sheet disintegrates into liquid ligaments and finally into liquid drops so that the drop size and its distribution, which are important for analyzing the combustion fields of liquid rocket engines, is determined by the sheet breakup. Therefore, understanding of the sheet breakup is a key for investigating the spray characteristics of impinging type injectors. Hence, extensive experimental and analytical researches have been carried out on the spray characteristics of the injector, especially, the breakup of liquid sheets formed by the impingement of two liquid jets [2-9].

Swirl type injectors have many advantages such as good atomization, low combustion instability and wide operating range because of its hydraulic spray characteristics [10]. Hence, it has been widely used in rocket engines, air-breathing engines and industrial drying, even though a swirl injector is more

* School of Mechanical and Aerospace Engineering, Seoul National University

difficult to design and manufacture than any other injector including a simple plain injector. The circumferential flow can be generated by using a screw or a set of tangential inlets in a swirl chamber. As the circumferential flow approaches to discharge orifice, it accelerates due to the shrink of orifice diameter. Due to high tangential flow velocity, a gas core is formed around the centerline inside the injector to balance the static pressure of the working fluid and the ambient pressure. At the injector exit, the liquid is injected at a specific spray angle, which in practice, corresponds to the ratio of the axial and tangential velocities. Further downstream, the injected liquid becomes thin and disintegrates into droplets by the hydrodynamic instability. And the discharge coefficient of a swirl injector is generally low and its spray cone angle is high.

Although the effects of the injection conditions and geometries on the breakup characteristics have been widely investigated during several decades, the experiments have been confined to atmospheric conditions. In practical liquid rocket engines, combustion occurs at a very high pressure, and it has been reported that the spray characteristics at high pressure conditions were much different from those at atmospheric conditions by Strakey & Talley [9]. In this study, the breakup characteristics of liquid sheets formed by the impinging and swirl type injectors were studied as increasing the Weber number (or injection condition) and the ambient gas pressure.

2. LIQUID SHEET BREAKUP

2.1 Linear Instability Theory

Linear instability theory, which is based on the growth of waves due to the aerodynamic force on the liquid sheet surface, has been used to describe the disintegration of liquid sheets. The aerodynamic instability of liquid sheet has been investigated on the basis of the Kelvin-Helmholtz instability [11][12]. Squire [11] was the first to investigate theoretically the instability of an inviscid liquid sheet of constant thickness. He considered two modes of disturbances: symmetric and anti-symmetric modes. And, he found that the anti-symmetric mode dominated the growth of disturbances. This conclusion was later validated by extensive studies [12].

Consider a two-dimensional, inviscid, incompressible liquid sheet of thickness $2h_0$ moving with velocity u through the quiescent ambient gas. The liquid and gas densities are ρ_l and ρ_g, respectively and the surface tension of liquid is σ. As the liquid sheet moves along the coordinate z, the liquid surface is disturbed. The disturbance on the liquid sheet surface is represented by η as follows:

$$\eta = \eta_0 \exp i(kz - \beta t) \qquad (1)$$

where η_0 is the initial amplitude of disturbance and β is the growth rate. Typically β is calculated for a spectrum of k. The disturbance wave number k_{max} corresponding to the maximum growth rate β_{max} controls the breakup process. If the surface disturbance has reached the critical wave amplitude at breakup, η_b, the breakup time can be calculated. The maximum growth rate is approximated as Eq. (2) and then the corresponding breakup length z_b can be given by Eq. (3) [12][13].

$$\left(\frac{\beta h}{u}\right)_{max} = \frac{\rho}{2}\sqrt{\frac{\rho_l u h}{\sigma}} = \frac{\rho}{2} We^{1/2} \qquad (2)$$

$$z_b = u t_b = \frac{u}{\beta_{max}} ln\left(\frac{\eta_b}{\eta_0}\right) \qquad (3)$$

where ρ is the density ratio of gas to liquid. Unfortunately, the theory does not predict a critical wave amplitude for sheet breakup η_b, and an empirical relation, $\ln(\eta_b/\eta_0)$= 12, has been generally used [12]. However, some investigators reported that $\ln(\eta_b/\eta_0)$ is not an universal value and has to be determined experimentally in every case. In this study, we just interested in the change of the breakup length according to the injection and ambient conditions.

2.2 Impinging Type Injectors

According to the stationary wave theory [2-4], which consider the mass and momentum balances between two liquid jets and a sheet, the breakup length is proportional only to the jet Weber number as following [4]:

$$x_b = 0.25\,We_j \quad (\text{when } \phi=30°) \tag{4}$$

where the jet Weber number We_j means the ratio of the jet inertial fore to the surface tension force, thus the sheet breakup length increases as increasing the injection velocity, irrespective of ambient gas density.

However, the stationary wave theory can be applied only when the injection velocity is low because the aerodynamic force of ambient gas affects the sheet breakup when the injection velocity is high. The effect of aerodynamic force is considered in the linear instability theory [5-7]. Huang suggested a semi-empirical relation based on an analysis for a vibrating membrane as following [6]:

$$\frac{x_b}{d_0} = 7.1\rho^{-2/3}We_j^{-1/3} \tag{5}$$

and Ryan et al. suggested the breakup length of liquid sheet formed by two impinging jets as following [7]:

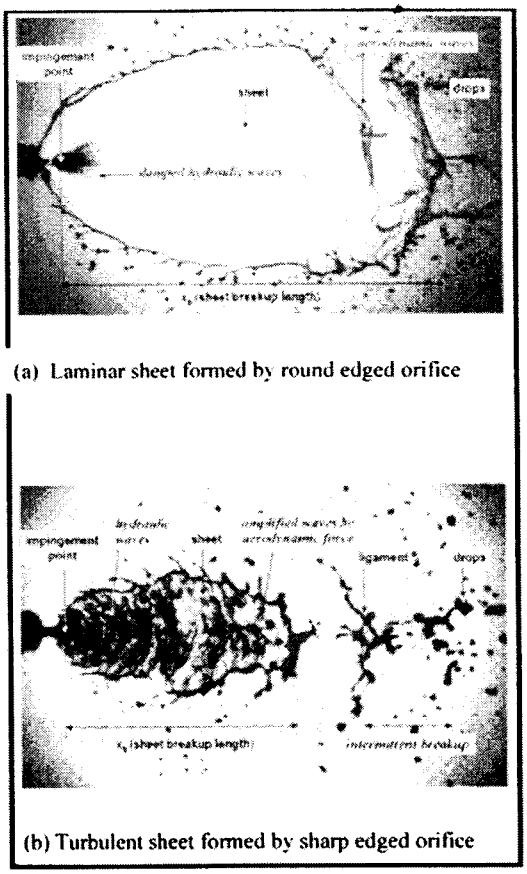

(a) Laminar sheet formed by round edged orifice

(b) Turbulent sheet formed by sharp edged orifice

Fig. 1 Comparison between laminar and turbulent sheets at the same condition (P_c=0.4MPa, U_j=7m/s).

$$\frac{x_b}{d_0} = 10.4\rho^{-2/3}We_j^{-1/3} \quad (\text{when } \phi=30°) \tag{6}$$

where the density ratio ρ means the ratio of ambient gas density to liquid sheet density, thus the breakup length decreases as increasing the ambient gas density or the jet injection velocity.

However, the breakup length obtained by the linear instability theory has shown disagreements with practical experiments because the theory did not consider the effects of the hydraulic force of impinging jets on the sheet breakup [7]. Dombrowski and Hooper reported that the flow characteristics of liquid jets, which is

dominated by the shape of orifice entrance and the jet velocity, strongly affect both the formation and breakup of liquid sheet [8]. When two liquid jets impinge and form a sheet, hydraulic waves are formed on the sheet but the waves are damped by the boundary layers if the jets are laminar. As for the turbulent jets that have no boundary layer, however, the hydraulic waves are not damped and strongly affect the sheet breakup. Thus, the laminar sheet formed by the laminar jets (Fig. 1(a)) is wider and flatter than the turbulent sheet formed by the turbulent jets (Fig. 1(b)) at the same injection velocity and ambient gas density. Recently, Strakey and Talley reported that the impact force determines the sheet breakup when the ambient gas density is low while the aerodynamic force determines the sheet breakup when the ambient gas density is high, but they did not suggest a quantitative result for the sheet breakup [9]. In present study, we compared the breakup characteristics between the laminar and turbulent sheets to investigate the effects of hydraulic force of turbulent jets. Also, we suggested empirical relations on the breakup lengths of both sheets, which are defined as the distances from the impingement point to the edge of liquid, x_b in Figs. 1(a) and (b).

2.3 Swirl Type Injectors

The spray shapes form impinging type injectors are flat liquid sheets, while those from swirl type injectors are conical liquid sheets with empty space around the centerline as shown in Fig. 2. In the case of the impinging type injector, the breakup length has been normalized as the orifice diameter d_0 like as Eq. (5) and (6) by simply letting $h=Cd_0^2/x_b$ [6]. However, in the case of the swirl type injector, the breakup length has been normalized as initial film thickness h_0, because a gas core is formed around the centerline inside the orifice. Therefore, he normalized breakup length relation based on the linear instability theory can be obtained as follows:

$$\frac{2_b}{h_0} = Cp^{-1}We^{-1/2} \tag{7}$$

Han et al. [14] proposed a semi-empirical relation to predict the breakup length of conical liquid sheet, based on the non-linear analysis of planar liquid sheet breakup by Clark and Dombroski [15].

$$L_b = C\left[\frac{\rho_L\sigma(\eta/\eta_0)h_0\cos\theta}{\rho_g^2U_L^2}\right]^{0.5} \tag{8}$$

where C is an experimental constant, set to 3 by them and is the spray angle.

However, the breakup length of conical spray obtained by the linear instability theory has shown disagreements with practical experiments because the theory did not consider the attenuation of sheet thickness. Dombrowski and Hooper [12] attempted to solve the breakup of the attenuating sheet, but their assumption was flat liquid sheet. As for the swirl type injectos, we also investigated the effect of ambient gas density on the spray shape and breakup characteristics of a swirl injector by measuring the breakup length. Since the breakup of a swirl spray is mainly controlled by the aerodynamic forces between the liquidsheet and ambient gas, the axial Weber number We_l(or sheet velocity) is also considered as an experimental variable. The main objective of the present study is to understand thespray patterns and the breakup phenomenon, which have an important influence on the atomization process, at high ambient pressures and relatively low injection pressures of a swirl injector. Also, we investigated whether the linear instability

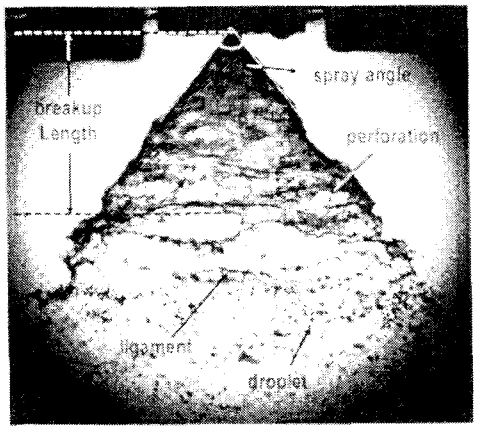

Fig. 2 Spray shape of swirl type injector

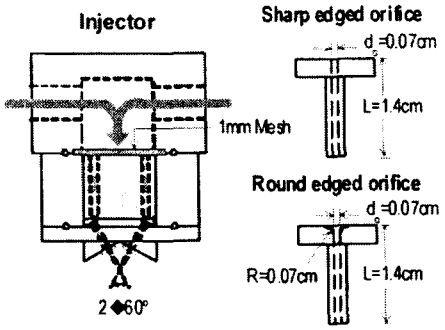

(a) Schematic of impinging type injector

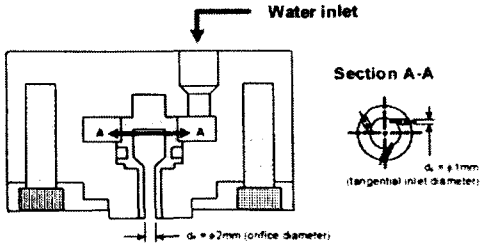

(b) Schematic of Swirl type injector

Fig. 3 Schematics of impinging and swirl type injectors

theory, which can describe the disintegration of liquid sheets, could be applied to the swirling annular sheets.

3. EXPERIMENTAL METHODS

3.1 Impinging Injectors

In order to obtain the laminar and the turbulent sheet, we designed round and sharp edged orifices as shown in Fig. 3(a). Since the orifice of whichentrance is rounded with 0.14 times of orifice diameter or much has no a vena contracta and forms a laminar jet [16], the round edged orifice was designed to have a curvature radius of one diameter of orifice. All the orifice diameters were 0.07*cm* and the ratios of orifice length to diameter were designed as 20, which is higher than those of practical impinging type injectors, in order to induce more steady flow. The impingement point of two liquid jets was fixed at the location of five times of orifice diameter from the orifice exit, and the impingement angle of two liquid jets was designed as 60 degrees. The discharge coefficient of round edged orifice (0.76) was higher than that of sharp edged orifice (0.69). It is general that the cavitation bubbles occur inside the sharp edged orifice, which reduces the discharge coefficient [17], but the decrease of discharge coefficient was not found in the present orifices. Thus, we did not consider the cavitation that affects the spray characteristics [18].

3.2 Swirl Injectors

The swirl injector, used in the experiments, was designed according to the hydraulics of Bayvel and Orzechowski [19] as shown in Fig. 3(b). The orifice diameter d0 was 2 mm and the tangential inlet had 3 holes with the diameter dp of 1 mm at every 120 degree. The injector was designed as a closed type having the separated vortex chamber and orifice, and the contraction ratio of the vortex chamber diameter to the orifice diameter was set to 3. Table 1 shows the experimental conditions and parameters. The injection

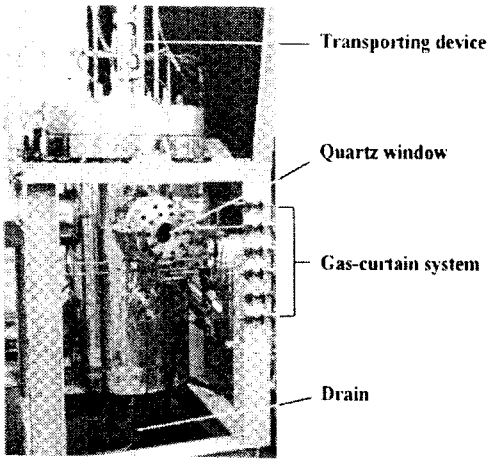

(a) High pressure chamber (Max. P = 6 Mpa)

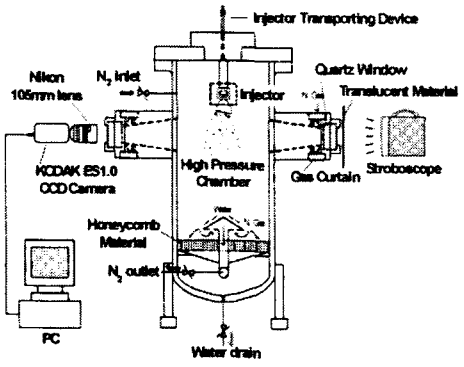

(b) Schematic of experimental apparatus

Fig. 4 Schematics of high pressure chamber.

pressure differential was varied from 0.061 to 0.579 MPa, which corresponds to the mass flow rate range of 8.73 to 25.51 g/s, respectively. Also, the axial Weber number Wel, whose definition will be introduced in the next section, was calculated according to the injection pressure and the experimental results are expressed in Wel, hereafter.

3.3 Experimental Methods

The high pressure chamber in Fig. 4 was designed to be pressurized with nitrogen gas up to 6MPa. The diameter and volume of chamber is 500mm and 200l, respectively. The transporting device on the chamber cover was set to move the injector under pressurized conditions and the gas curtain system was designed to remove the deposition of fine spray drops on the quartz windows, which obstructs the spray visualization.

We measured the sheet breakup length from the instantaneous spray images taken by indirect photography as shown in Fig. 4(b). A stroboscopic light of which luminous time is less than $4\mu_s$ was illuminated on a translucent material. The exposure time of a camera (KODAK ES1.0) was set to be identical to the flash interval of stroboscope to take an image per a flash without an extra synchronization. One hundred images were measured and averaged for one experimental case, and the deviations of data were less than 10 percents of their mean values.

4. RESULTS AND DISCUSSION

4.1 Impinging Injectors

The injection velocity, which determines the aerodynamic force and the impact force, and the ambient pressure (i.e. ambient gas density), which determines the aerodynamic force, were chosen as experimental variables. These two variables could be non-dimensionalized with the jet Weber number We_j ($=\rho_l U_j^2 d_o/\sigma$) and density ratio ρ ($=\rho_g/\rho_l$), respectively, because the liquid density, the surface tension and the orifice diameter were constant. Also, we used the gas based Weber number We_g to consider both variables with one parameter as following:

$$We_g = \rho We_j = \frac{\rho_g U_j^2 d_0}{\sigma} \tag{9}$$

According to the definition, We_g means the ratio of aerodynamic force of ambient gas to surface tension force of liquid sheet, thus We_g increases as the injection velocity or the ambient gas pressure increases.

(1) Laminar Sheet Breakup

Figure 5 shows the effects of ambient gas pressure P_c and injection velocity U_j on the shapes of laminar sheets formed by the round edged orifices. First of all, it was found that the laminar sheet, which damps the impact waves, is not shown above the injection velocity of $15m/s$ or the jet Weber number of about 2,000. The reason is thought that the impact force is too strong for the jet boundary layer of low velocity to damp after the velocity. Therefore, we regarded the sheet of which velocity is lower than $15m/s$ as the laminar sheet.

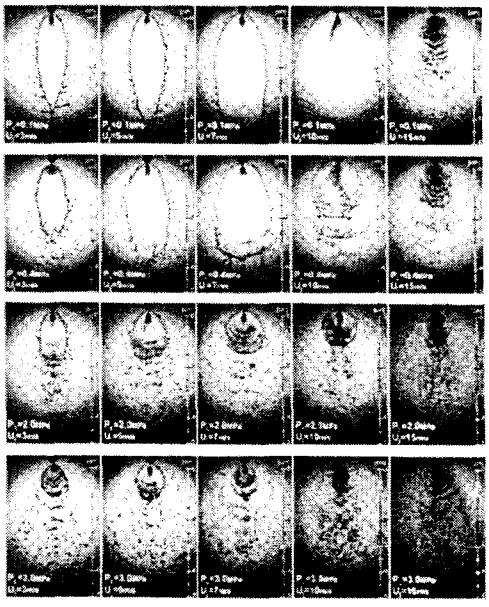

Fig. 5 Changes of laminar sheet shapes as functions of injection velocity and ambient pressure.

It is interesting that the laminar sheets expand as increasing the injection velocity until the ambient pressure is $0.4MPa$. In this condition, the impact waves, which were formed by the impingement of two liquid jets, damped so that any waves do not appear on the sheets. As increasing the ambient pressure, another waves appear before the sheet breakup as shown in the sheet images at the ambient pressure of $2MPa$, and these waves result from the increase of aerodynamic force of ambient gas. Although these aerodynamic waves cause the sheet breakup by attenuating the sheet thickness, they do not form a liquid ligament and the sheets are broken into the drops directly. Thus the intermittent spray pattern, which has known as an important spray characteristic of impinging type injectors, does not appear.

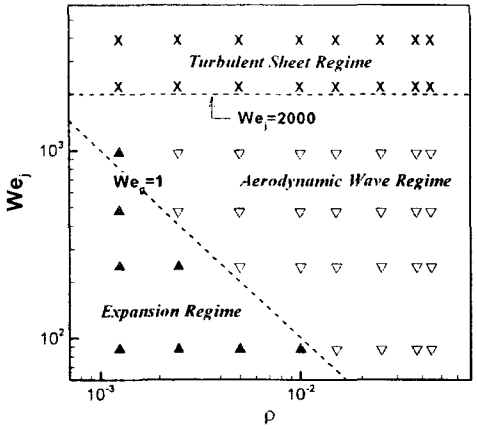

Fig. 6 Breakup criteria of laminar sheet: and were marked when the aerodynamic waves do not appear and appear on the sheet, respectively, and X were marked when the laminar sheet does not exist.

From Fig. 5, the breakup criteria of laminar sheet could be obtained as shown in Fig. 6. The symbols ▲ and ▽ were marked according to the existence of aerodynamic waves on the sheet. It was found that the laminar sheet has two breakup regimes. First, the sheet expands due to the increase of injection mass flow rate as increasing the jet velocity when We_g is lower than about unity. Although the aerodynamic force of

ambient gas also increases as increasing the injection velocity, the aerodynamic force is too weak to form the aerodynamic waves in the conditions. If the aerodynamic force becomes higher than the surface tension force of sheet, i.e. We_g is higher than unity, the aerodynamic waves appear on the sheet. Although the impact waves are damped in both the expansion regime and the aerodynamic wave regime, the hydraulic force of two impinging jets becomes too strong to be damped after the jet Weber number is higher than 2000, and thus the laminar sheet

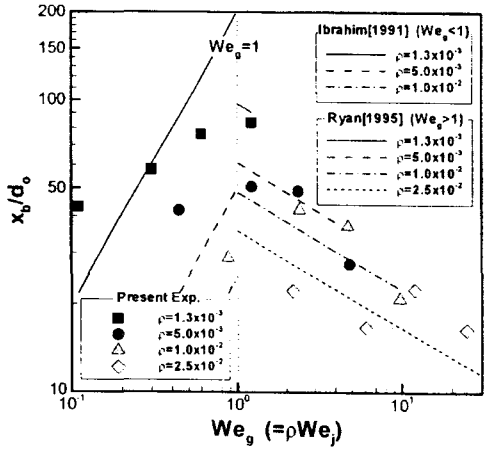

(a)

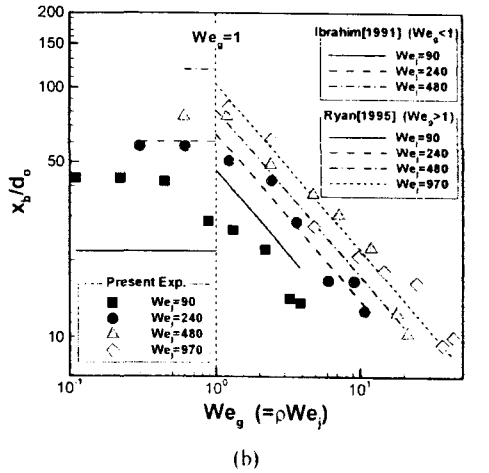

(b)

Fig. 7 Breakup lengths of laminar sheets as a function of Weg: (a) jet Weber number Wej and (b) density ratio of gas to liquid .

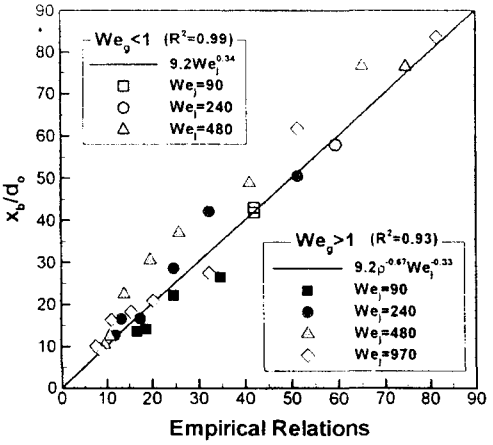

Fig. 8 Empirical relation on the breakup length of laminar sheet.

cannot appear after the Weber number. It is interesting that the criterion between laminar and turbulent sheets depends on only the injection velocity irrespective of the ambient gas density.

Figure 7 shows the breakup lengths as a function of We_g. Figure 7(a) shows the breakup lengths as increasing the jet Weber number at the constant ambient gas density and Fig. 7(b) shows the breakup lengths as increasing the ambient gas density at the constant jet Weber number. The most interesting finding is that the breakup length shows a definitely different tendency before and after $We_g$is about unity. In the cases that $We_g$is lower than unity, the aerodynamic force which induces the sheet breakup is so weak that the sheet expands due to the increment of mass flow rate as increasing the jet Weber number We_j as shown in Fig. 7(a). However, the breakup length was not proportional to We_j, which is expected by the stationary wave theory of Eq. (4), but to $We_j^{0.34}$. Thus it is thought that the stationary wave theory overestimates the sheet expansion. Also, Fig. 7(b) shows the breakup lengths are not significantly changed as increasing the ambient gas density when

We_g is lower than unity. In the cases that We_g is higher than unity, however, the sheets are broken by the aerodynamic force. Since the laminar sheet damps the effect of hydraulic force on the sheet breakup, the sheet breakup are dominated by only the aerodynamic force, and thus the breakup lengths agree well with the linear instability theory of Eqs. (5) and (6) that considers the effects of aerodynamic force except the effects of hydraulic force.

Using the results of Fig. 7, an empirical relation on the breakup length of laminar sheet could be obtained as following:

$$\frac{x_b}{d_0} = 9.2\,We_j^{0.31} \quad (We_g < 1) \qquad (10)$$

$$\frac{x_b}{d_0} = 9.4\rho^{-2/3}\,We_j^{-1/3} \quad (We_g > 1,\ We_j < 2000)$$

In the case that We_g is higher than unity, the indexes of parameters of above equation are same with the linear instability theory, but the constant 9.4 is in between 7.1 of Eq. (5) and 10.4 of Eq. (6). Figure 8 shows the comparison between the experimental results and the following empirical relation.

(2) Turbulent Sheet Breakup

Figure 9 shows the effects of ambient gas pressure P_c and injection velocity U_j on the shapes of turbulent sheets formed by the sharp edged orifices. In the turbulent sheets, the waves exist on the sheet in all experimental conditions because the hydraulic waves are not damped. Since the hydraulic waves can be easily amplified by the aerodynamic force, it is expected that the breakup length of turbulent sheet is shorter than that of laminar sheet at the same condition. Although the turbulent sheets have the hydraulic waves formed by the impingement of two jets irrespective of Weg, the waves do not contribute the sheet breakup at the low We_g, e.g. when U_j=3 or 5m/s at P_c=0.1MPa. In the case, the intermittence of drop formation is not shown. Also, the breakup length can not be defined in the case of very high We_g, e.g. when P_c=2.0 or 4.0MPa at U_j=30m/s. Figure 10 shows these breakup criteria of turbulent sheets. The symbols ▲ and ▽ were marked according to the existence of the spray intermittence.

From Fig. 10, it was found that the turbulent sheet has three breakup regimes. First, the sheet breakup is not controlled by waves so that the intermittent breakup does not appear and the breakup length increases as increasing the injection velocity when Weg is lower than about 2. Although this sheet expansion regime is also found in the laminar sheet, the criterion of turbulent sheet (We_g=2) is higher than that of laminar sheet (We_g=1). The reason is thought that since the sheet thickness of turbulent sheet is waves on the turbulent sheet is lower than that of laminar sheet, thus the aerodynamic force can affect the sheet breakup at the higher We_g. As We_g increases, the

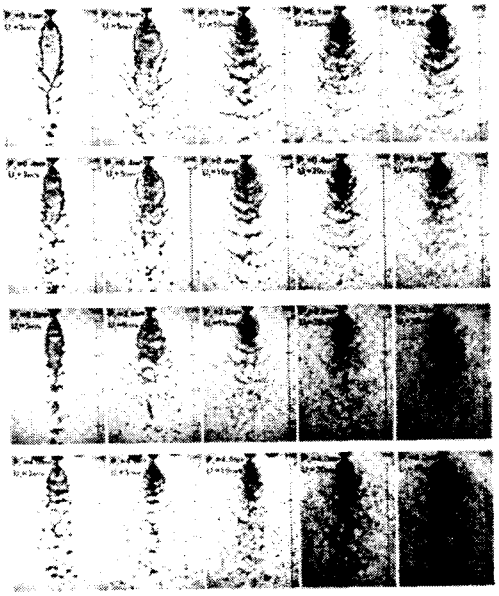

Fig. 9 Changes of turbulent sheet shapes as functions of injection velocity and ambient pressure.

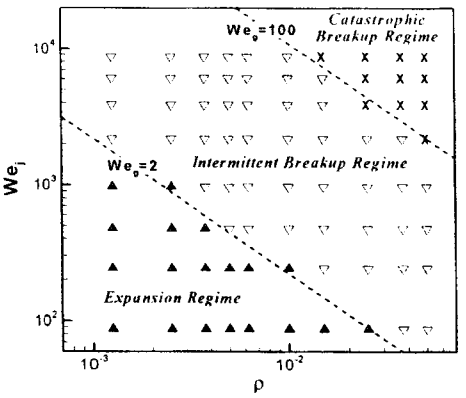

Fig. 10 Breakup criteria of turbulent sheet: ▲ and ▽ were marked when the spray intermittence does not appear and appears, respectively, and X were marked when the breakup length could not be measured.

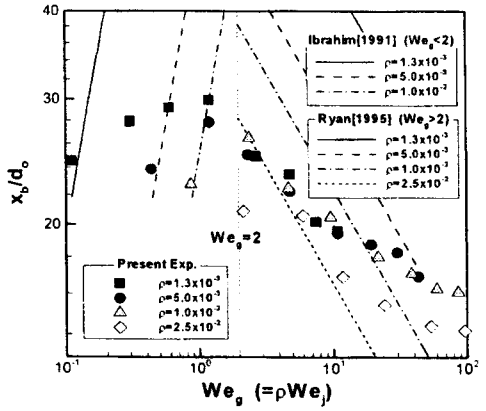

(a)

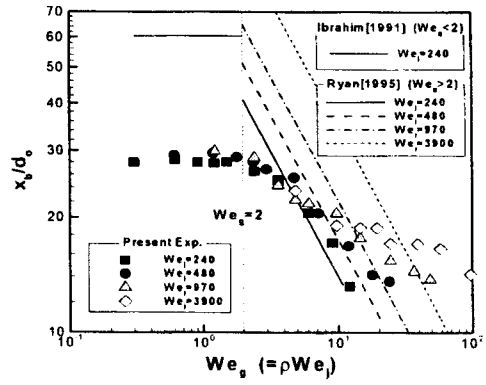

(b)

Fig. 11 Breakup lengths of turbulent sheets as a function of We_g: (a) jet Weber number We_j and (b) intermittent breakup regime where the , the density ratio of gas to liquid ρ.

intermittent breakup regime where the turbulent sheet breakup is determined by the growth of waves appears until We_g is lower than 100. Since the sheets are broken by the hydraulic waves amplified by the aerodynamic force spray intermittence appears. After We_g is higher than 100, the sheets are broken just after injection by the strong aerodynamic force so that the breakup length can not be discriminated in this catastrophic breakup regime.

Figure 11 shows the breakup lengths of turbulent sheets as a function of We_g. As shown in Fig. 11(a), the breakup lengths increase as increasing the jet Weber number when We_g is lower than 2. In this expansion regime, the aerodynamic force does not affect the turbulent sheet breakup as shown in Fig. 11(b). Further increase of We_g, the hydraulic waves are grown by the aerodynamic force so that the breakup length decreases. The linear instability theory expects that the breakup length is proportional to $\rho^{-0.67}$ However, the effect of ambient gas density on the breakup length becomes mitigated from $\rho^{-0.42}$ at We_j=240 to $\rho^{-0.13}$ at We_j=3900 as the jet Weber number increases. This can be explained by the effect of the hydraulic force. As the injection velocity increases, the hydraulic force becomes so strong that the amplitudes of waves are high enough to break the sheet without the amplification by the aerodynamic force. Therefore, the effect of ambient gas pressure is dependent on the injection velocity, i.e. the jet Weber number.

From the results of Fig. 11, an empirical relation on the breakup length of turbulent sheet could be obtained as following:

$$\frac{x_b}{d_0} = 15.3\,We_j^{0.098} \quad (We_g < 2) \tag{11}$$

$$\frac{x_b}{d_0} = 0.61\rho^{-1.63\,We_j^{-0.31}}\,We_j^{0.31} \quad (2 < We_g < 100)$$

where $We_j^{0.31}$ was used We_j to compensate

the effect of We_l in $\rho^{-4.63ej-0.41}$ and it does not have a physical meaning. Figure 12 shows the comparison between the experimental results and the empirical relation.

4.2 Swirl Injectors

(1) Spray Patterns

Figure 13 shows the effects of the axial Weber number We_l (or injection condition) and ambient gas pressure Pc on the swirling liquid spray patterns. As the We_l increases, spray shape undergoes a tulip stage and grows to a fully-developed cone due to the increase of tangential velocity. Also, the disturbances on the liquid sheet surface are amplified by the increase of sheet velocity, and thus, the annular liquid sheet with higher We_l breaks up near from the injector exit. As the ambient gas pressure increases, the disturbed wavelength on the liquid sheet surface decreases and the annular liquid sheet breaks up faster, due to the increase of the aerodynamic drag. Hence, the sheet breaks up when the film is thicker, so that the atomized droplets seem to be larger than those of lower ambient gas pressure. At higher ambient gas pressure and larger mass flow rate, the sprays were dense due to the atomized droplets. To observe the effect of ambient gas pressure, the spray distributions perpendicular to the injection direction were measured by the optical line patternator. The measurements were conducted at 30*mm* from the injector exit as the ambient gas pressure was increased, but the injection condition was maintained at We_l = 1157. The spray distribution of atmosphere ambient condition shows the typical hollow cone shape. As the ambient gas pressure increased, however, the spray width became narrower. And the atomized small droplets penetrated into the center of the injector by the entrained ambient gas so that the spray shape changed from a wide hollow cone to a narrow solid cone.

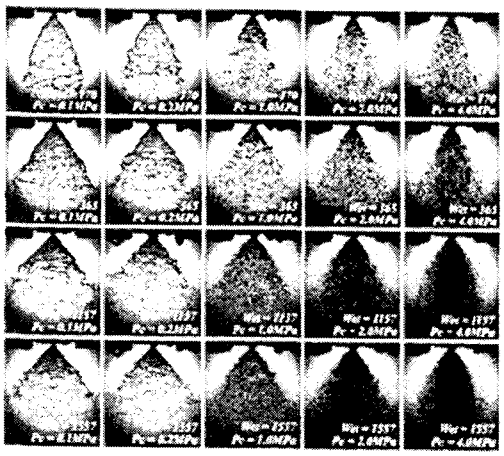

Fig. 13 Spray patterns of swirling liquid sheets according to the axial Weber number Wel and ambient gas pressure

(2) Measured Breakup Length

The breakup of annular liquid sheets emerging from a swirl injector undergoes a complex, unsteady, non-linear process. The breakup initiates at the side of liquid sheet along its length in series of circular ligaments or distorted ligament-like structures [10]. From the Fig. 13, the breakup at We_l = 170 seemed close to the distorted ligament-like structure; however, in all cases of the present injection conditions, it does not matter to regard that the liquid sheets were disintegrated into ligaments and droplets. There exist several possible criteria of breakup length definition in the literatures. In present study, the breakup length of the swirling liquid sheet is defined as the distance from the orifice exit where droplets form. Sixty images were measured for one experimental case, and the deviations of data were less than 10 percents of their mean values. However, the breakup length at the

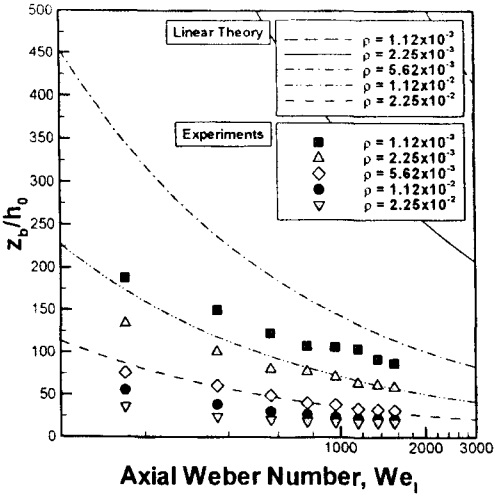

(a)

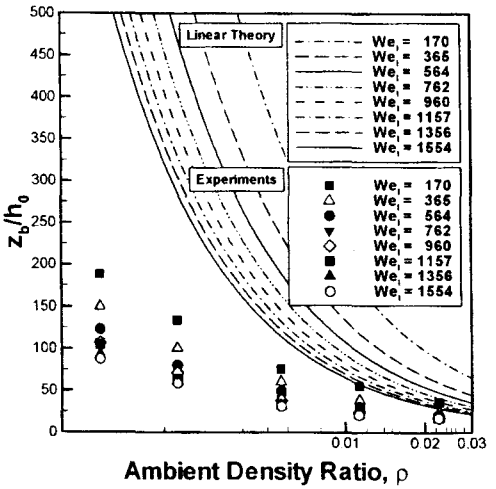

(b)

Fig. 14 Breakup length of swirling liquid sheets according to (a) axial Weber number, We_l (b) ambient gas density ratio of gas to liquidρ .

ambient gas pressure of 4.0MPa cannot be measured due to the very dense spray.

Figure 14 shows the breakup lengths of a swirling liquid sheet according to the axial Weber number and ambient density ratio of gas to liquid. The breakup lengths were normalized by the initial sheet thickness h_0, which was varied only with the injection condition (or We_l).

Figure 14(a) shows the effects of the axial Weber number We_l on the breakup lengths, and Fig. 14(b) indicates the effects of ambient gas density ratio of gas to liquid on the breakup lengths. And the linear instability theory and experimental data were compared. As confirmed in the spray images of Fig. 13, the breakup length decreases when the aerodynamic force increases as the ambient gas density and Wel increase. The decrease of breakup length according to the increase of Wel can be explained by two factors. First, the liquid film thickness decreases with the injection pressure, and thus the annular liquid sheet breaks easily. Second, the disintegration of annular liquid sheet is promoted by aerodynamic effects.

Figure 14 shows the difference of breakup length between experiments and linear instability theory. The theory itself cannot predict a critical wave amplitude for the breakup ≈b, as stated above; hence, the term ln(≈b /≈0) is

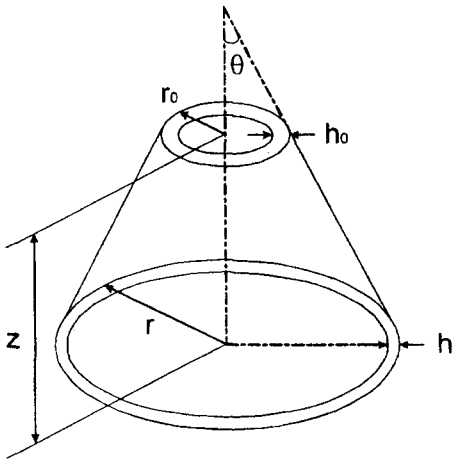

Fig. 15 The schematics of sheet thickness change in a annular liquid sheet.

given in the present study based on the work of Dombrowski and Hooper [12][13]. Since the critical wave amplitude for breakup is introduced from the empirical relation for the disintegration of planar liquid sheet, this

value can be discrepant from the annular swirling liquid sheet. The linear instability theory predicts the variation of breakup length as $We^{-0.5}$, but present experimental data indicates that it is proportional to $We^{-0.38}$. Moreover, the dependence of the normalized breakup length on the density ratio is not $\rho^{-1.0}$ by the linear instability theory, but $\rho^{-0.59}$. In practice, liquid sheet, discharged from the injector, is attenuated as it moves away from its origin, but for the simplicity, the instability theory for a sheet whose thickness remains constant has been developed. We believe that the main reason for the disagreement of experimental data with the linear instability theory is due to the effect of the change in the liquid sheet thickness on the sheet breakup mechanism. Dombrowski and Hooper [12] attempted to solve the breakup of the attenuating sheet, but their assumption was different from the present swirling liquid sheet.

For a conical liquid sheet, the schematic of sheet thickness change is described as shown in Fig. 15. By assuming a mass flow rate at each perpendicular plane, the change in the sheet thickness as a function of the distance from the injector exit z and the spray angle θ could be calculated. As stated in the previous section, the spray angle before breakup is independent of the ambient gas density and is only a function of We_l. Since $z=ut$, h could be finally expressed with time as shown in Eq. (12). h_0 is the film thickness at the injector exit and r_0 is the orifice radius.

$$h = \frac{h_0 r_0}{r_0 + z\tan\theta} = \frac{h_0 r_0}{r_0 + Ut\tan\theta} \qquad (12)$$

And thus, the growth rate must be integrated over the breakup time, so that the total growth of the wave is used to predict the breakup length as in Eq. (13). As a result, the corrected linear instability theory considering the attenuation of sheet can be obtained as shown in Eq. (14) and the developed equation is more complex.

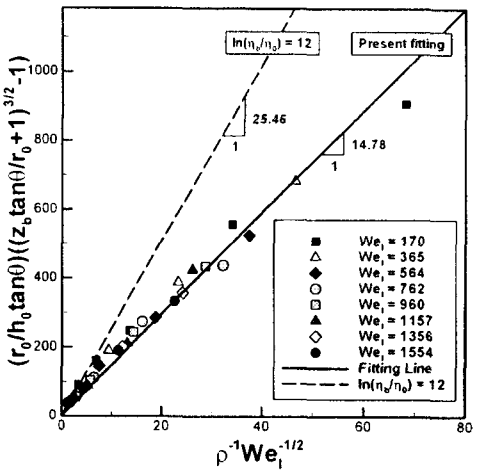

Fig. 16 The comparison of breakup lengths between our experiment and corrected linear instability theory considering the attenuated sheet thickness.

$$\ln\left(\frac{\eta_b}{\eta_0}\right) = \int_0^{t_b} \beta_{max}\, dt \qquad (13)$$

$$\left(\frac{r}{h\tan\theta}\right)\left[\left(\frac{z\tan\theta}{r}+1\right)^{3/2}-1\right] = C\rho^{-1}We_l^{-1/2} \qquad (14)$$

Figure 16 shows the comparison of the breakup lengths with the corrected linear instability theory considering the attenuated sheet thickness. The constant C on the right side of Eq. (14) was determined as 14.78 from experimental data and the dashed line in Fig. 16 indicates the values calculated from $ln(\eta_b/\eta_0)=12$. These two lines show some discrepancy. Many studies on the breakup phenomena of liquid jet and sheet state that $ln(\eta_b/\eta_0)=12$ is a universal constant and can be applied to any geometrical configuration, but it seems that the term has to be determined from experiments. As a result, the newly developed equation predicts well the breakup length of swirling annular liquid sheet.

5. CONCLUSIONS

The results of the measurements of spray characteristics of impinging type injectors under the high ambient pressure showed that the aerodynamic force significantly affects the breakup of laminar sheet when the aerodynamic force is higher than the surface tension force, i.e. We_g is higher than unity. When We_g is lower than unity, however, the laminar sheet expands as increasing the injection velocity and the aerodynamic force does not affect the sheet breakup.

The breakup characteristics of turbulent sheets had three regimes, i.e. expansion regime, intermittent breakup regime and catastrophic breakup regime according to We_g. Under the expansion regime, the sheet breakup length increases as increasing the injection velocity and the aerodynamic force does not affect the breakup length. Under the intermittent breakup regime, the breakup length decreases as increasing the injection velocity or the ambient gas density due to the aerodynamic force. However, the effect of aerodynamic force becomes mitigated as increasing jet Weber number. Under the catastrophic breakup regime, the breakup length could not be discriminated.

The measurements of breakup length of swirl type injectors under high ambient pressure showed that the breakup length decreased with increasing aerodynamic force as the ambient gas density and We_l increased. Also, it was found that the breakup lengths predicted by the corrected linear instability theory considering the attenuation of sheet thickness agree well with our experimental results.

6. NOMENCLATURE

d_o orifice diameter

L orifice length

P_c ambient gas pressure

R entrance curvature radius of round edged orifice

R_2 Square of Pearson's correlation coefficient

U_j jet injection velocity

We_j jet Weber number for impinging type injectors, $\rho_l U_j^2 d_o/\sigma$

Wel axial Weber number for swirl type injecors, $\rho_l u^2 h_o/\sigma$

Weg jet Weber number based on gas density, $\rho_g U_j^2 d_o/\sigma$

x_b sheet breakup length, i.e. distance from impingement point to sheet edge

Φ half impingement angle of liquid jets

ρ ratio of ambient gas density to liquid density

ρ_l liquid density

ρ_g ambient gas density

σ surface tension

r_0 orifice radius

h_0 nitial sheet thickness at injector exit

P_c ambient gas pressure

u axial velocity

β growth rate of wave

ΔP injection pressure difference

η_b amplitude of wave at breakup

η_i initial amplitude of wave at the injector exit

Θ spray half angle

7. REFERENCES

1. G. S. Gill and W. H. Nurick, Liquid Rocket Engine Injectors, NASA Technical Rep. SP-8089, 1976.

2. G. I. Taylor, Formation of Thin Flat Sheets of Water, Proceedings of the Royal Society of London A, Vol. 259, pp. 1-17, 1960.

3. D. Hasson and R. E. Peck, Thickness Distribution in a Sheet Formed by Impinging Jets, A.I.Ch.E. Journal, pp. 752-724, 1964.
4. E. A. Ibrahim and A. J. Przekwas, Impinging Jets Atomization, Physics of Fluids A, vol. 3, pp. 2981-2987, 1991.
5. H. B. Squire, Investigation of the Instability of a Moving Liquid Film, British Journal of Applied Physics, vol. 4, pp. 167-169, 1953.
6. J. C. P. Huang, The Break-Up of Axisymmetric Liquid Sheets, Journal of Fluid Mechanics, vol. 43, no. 2, pp. 305-319, 1970.
7. H. M. Ryan, W. E. Anderson, S. Pal and R. J. Santoro, Atomization Characteristics of Impinging Liquid Jets, Journal of Propulsion and Power, vol. 11, no. 1, pp. 135-145, 1995.
8. N. Dombrowski and P. C. Hooper, A Study of the Sprays Formed by Impinging Jets in Laminar and Turbulent Flow, Journal of Fluid Mechanics, vol. 18, no. 3, pp. 392-400, 1964.
9. P. A. Strakey and D. G. Talley, Spray Characteristics of Impinging Jet Injectors at High Back-Pressure, 8th ICLASS, 2000.
10. Lefevbre, A.W., "Atomization and Sprays", Hemisphere Publishing Corparation, 1989.
11. Squire, H.B., "Investigatin of the Instability of a Moving Liquid Film", British Journal of Applied Physics, Vol. 4, 1953, pp. 167-169.
12. Dombrowski, N. and Hooper, P.C., "The effect of Ambient Density on Drop Formation in Sprays", Chemical Engineering Science, Vol. 17, 1962, pp. 291-305.
13. Hagerty, W.W. and Shea, J.F., "A Study of the Stability of Plane Fluid Sheets", Journal of Applied Mechanics, 1955, pp. 509-514.
14. Han, Z., Parrish, S., Farell, P.V., and Reitz, R.D., "Modeling Atomization Processes of Pressure-Swirl Hollow-Cone Fuel Sprays", Atomization and Sprays, Vol. 7, No. 6., 1997, pp. 663-684.
15. Clark, C.J., and Dombrowski, N., "Aerodynamic Instability and Disintegration of Inviscid Liquid Sheets", Proc. Roy. Soc. Lond. A., Vol. 329, 1972, pp. 467-478.
16. J. K. Vennard, Elementary Fluid Mechanics, Wiley, New York, 1961.
17. W. H. Nurick, Orifice Cavitation and Its Effect on Spray Mixing, Journal of Fluids Engineering, Dec., pp. 681-687, 1976.
18. N. Tamaki, M. Shimizu, K. Nishida and H. Hiroyasu, Effects of Cavitation and Internal Flow on Atomization of a Liquid Jet, Atomization and Spray, vol. 8, pp. 179-197, 1998.
19. Bayvel, L. and Orzechowski, Z., "Liquid Atomization", Taylor & Francis, 1993.